

19,06

Thermophysical properties of multiferroics $\text{Bi}_{1-x}\text{Tm}_x\text{FeO}_3$

© S.N. Kallaev¹, A.G. Bakmaev¹, Z.M. Omarov¹, L.A. Reznichenko²¹ Institute of Physics, Dagestan Federal Research Center, Russian Academy of Sciences, Makhachkala, Russia² Southern Federal University, Rostov-on-Don, Russia

E-mail: kallaev-s@mail.ru

Received October 14, 2021

Revised October 14, 2021

Accepted October 18, 2021

Investigations of the heat capacity, thermal diffusivity, and thermal conductivity of multiferroics $\text{Bi}_{1-x}\text{Tm}_x\text{FeO}_3$ ($x = 0, 0.05, 0.10, 0.20$) have been carried out in the high temperature range of 300–1200 K. and thermal conductivity in the region of phase transitions. The temperature dependences of the specific heat for compositions with $x = 0.10$ and 0.20 exhibit an additional anomaly characteristic of the phase transition at $T = 580$ K. The dominant mechanisms of phonon heat transfer in the region of ferroelectric and antiferromagnetic phase transitions are considered. The temperature dependence of the average phonon mean free path is determined.

Keywords: multiferroics, heat capacity, thermal diffusivity, thermal conductivity.

DOI: 10.21883/PSS.2022.02.52979.221

1. Introduction

In recent years a great attention is paid to studies of materials where magnetic and electric orderings are implemented simultaneously (multiferroics). In these materials a magnetoelectric (ME) effect arises with which magnetization is regulated by the applied electric field or electric polarization is regulated by the magnetic field. Multiferroics, in particular the compounds based on bismuth ferrite, BiFeO_3 , are subject of intensive investigations, because these materials provide a wide range of applications, including data storage devices, spintronics, magnetoelectric sensor devices and multistable memory units. One of BiFeO_3 benefits are extremely high temperatures of ferroelectric (at $T_c \sim 1083$ K) and antiferromagnetic (at $T_N \sim 643$ K) ordering [1]. Bismuth ferrite at room temperature has spatial group $R3c$. Crystal structure is characterized by rhombohedrally distorted perovskite cell, which is very close to cube. In the range of temperatures below Neel point T_N bismuth ferrite possesses a complex spatially modulated magnetic structure of cycloid type, which does not allow the presence of ferromagnetic properties [2]. One of methods to destruct its spatially modulated spin structure that leads to emergence of the magnetoelectric effect is doping of bismuth ferrite with rare-earth elements. In this case the replacement by various rear-earth elements, as well as the increase in concentration of rear-earth ions result in changes in the phase composition of the formed compounds. The analysis of numerous publications devoted to investigations of ceramic BiFeO_3 modified with rear-earth elements shows that no consensus exists about the sequence of structural phase transitions and temperature ranges of existence of various phases at replacement by different rear-earth elements, as well as at changes in

their concentration. All this stimulates further detailed investigations of BiFeO_3 -based multiferroics doped with rear-earth elements.

$\text{Bi}_{1-x}\text{Tm}_x\text{FeO}_3$ ceramic compounds were investigated using structural, electric, and magnetic methods in a number of works [3,4]. As far as we know, thermophysical properties of $\text{Bi}_{1-x}\text{Tm}_x\text{FeO}_3$ have not been investigated at all. It should be noted that previously the studies of thermophysical properties of some compounds based on BiFeO_3 (with other rear-earth elements) were presented by us in a number of works [5–7].

This work reports the results of studies of heat capacity, temperature conductivity, and thermal conductivity of $\text{Bi}_{1-x}\text{Tm}_x\text{FeO}_3$ multiferroics in a wide range of temperatures: 300–1200 K, including the range of high-temperature phase transitions.

2. Specimens and experiment

The targets of the study were ceramic specimens of solid solutions of $\text{Bi}_{1-x}\text{Tm}_x\text{FeO}_3$ (where $x = 0, 0.05, 0.10, 0.20$). The ceramic was produced using the conventional ceramic technology of solid-phase synthesis followed by baking without applying pressure in the air atmosphere. The synthesis was performed by the method of solid-phase reactions of Bi_2O_3 , Fe_2O_3 , Tm_2O_3 high-purity oxides in two stages with intermediate milling and granulating of powders. Synthesis modes: temperature of the first baking $T_1 = 1073$ K ($\tau_1 = 10$ h), the second baking $T_2 = 1073$ – 1123 K ($\tau_2 = 5$ h). The powder properties required for pressing were attained by introducing plasticiser in them followed by granulating. Optimum temperature for the baking was selected by choosing

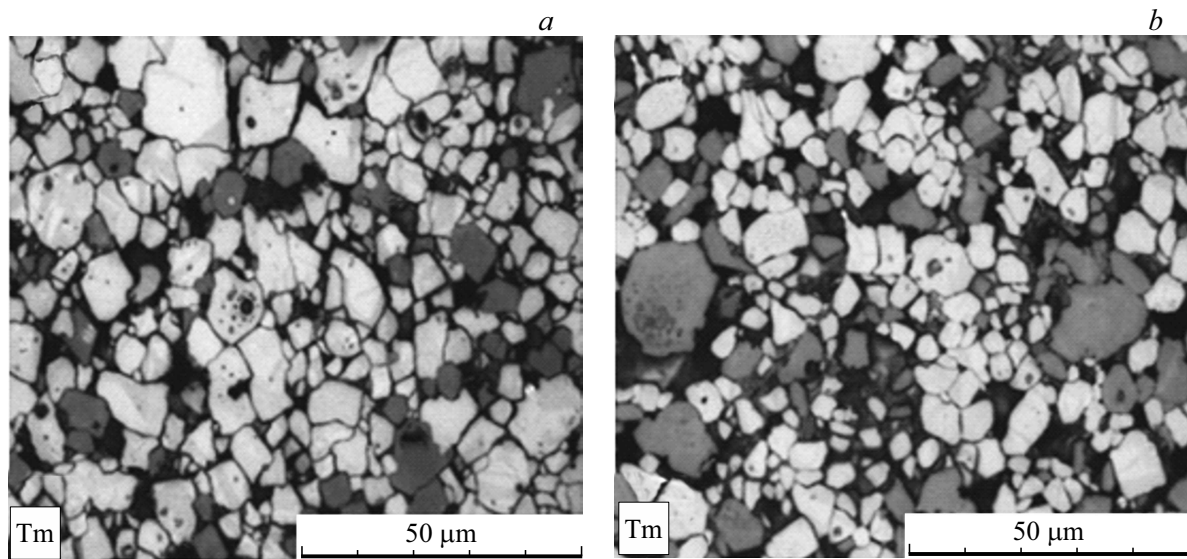


Figure 1. Microstructures of $\text{Bi}_{1-x}\text{Tm}_x\text{FeO}_3$ ceramic specimens: $x = 0.10$ (a) and $x = 0.20$ (b) at room temperature.

from different baking temperatures, T_b , in the range of 1173–1223 K. The electron microprobe analysis was conducted using ADP-1 diffractometer ($\text{CoK}\alpha$ radiation) in the temperature range of 300–1000 K. Phase composition, parameters of the cell, the degree of perfection of the crystal structure were determined. The resulted solid solutions had sufficiently high values of experimental and relative densities (89–94)% and complied with limit attainable values for the conventional ceramic technology (90–95)%,, which gives evidence of quite high quality of the ceramic products. X-ray phase studies have shown that all specimens contained impurity phases $\text{Bi}_{25}\text{FeO}_{40}$ ($a = 10.181 \text{ \AA}$, cubic symmetry) and $\text{Bi}_2\text{Fe}_4\text{O}_9$ (rhombic symmetry), accompanying the formation of BiFeO_3 [8].

The work is carried out with the use of equipment provided by the Equipment Sharing Center „Thermophysical Research Methods“ of the Institute of Physics of the Dagestan Federal Research Center of Russian Academy of Science. Temperature conductivity and thermal conductivity were investigated by laser flash method using LFA-457 MicroFlash setup by NETZSCH (Germany). The relative measurement error did not exceed 6%. Parallel-plane specimens were used: diameter 12.7 mm and thickness 1 mm. The temperature change rate was 5 K/min. No any additional coating was used during measurements. Thermal conductivity was calculated by the following formula: $\lambda = \eta C_p \rho$, where η — temperature conductivity, ρ — specimen density, C_p — heat capacity. Heat capacity was measured by DSC 204 F1 Phoenix[®] differential scanning calorimeter by NETZSCH. The specimen for heat capacity measurement was shaped as a plate with a diameter of four and a thickness of one mm, respectively.

3. Results and discussions

Figure 1 shows photos of microstructure of the investigated solid solutions of $\text{Bi}_{1-x}\text{Tm}_x\text{FeO}_3$, where $x = 0.10$ and 0.20. Pores can be seen — the dark areas of round and irregular shape. They are distributed over the surface in a non-uniform way. Crystal grain boundaries can be clearly seen: closed dark lines around lighter areas (grains of the ceramic) Also, gray areas are observed, which are most probably related to formation of impurity phases.

Figure 2 shows results of studies of the heat capacity C_p of $\text{Bi}_{1-x}\text{Tm}_x\text{FeO}_3$ solid solutions, where $x = 0, 0.05, 0.10, 0.20$ in the temperature range of 300–800 K. As can be seen from the figures, the temperature dependencies of heat capacity of all compositions have anomalies in the range of antiferromagnetic phase transition temperature T_N . Doping of bismuth ferrite by thulium results in increase in the heat capacity in a wide range of temperature above $T \geq 300 \text{ K}$ (Fig. 2). What is more, the thulium doping does not result in a noticeable shift of the transition temperature T_N .

The temperature dependencies of C_p for compositions of $x = 0.10$ and 0.20 show the second anomaly, which is typical for phase transition, at a temperature of $T \approx 580 \text{ K}$ (below T_N). It should be noted that in this temperature range we have also observed anomalies on the temperature dependence of dielectric permittivity for these compositions [9].

According to electron microprobe studies of $\text{Bi}_{1-x}\text{Tm}_x\text{FeO}_3$ [3,4], in compositions with $x \geq 0.10$ at room temperature two phases are implemented: rhombohedral phase $R3c$ and orthorhombic phase $Pnma$, therefore, it can be assumed that the anomaly of heat capacity at $T \approx 584 \text{ K}$ for the composition with $x = 0.10$ and 0.20 may be due to the structural phase transition between the rhombohedral and orthorhombic structures.

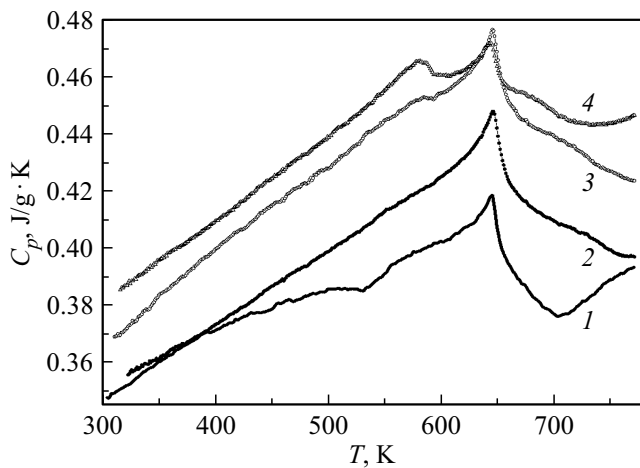


Figure 2. Temperature dependence of multiferroic heat capacity $\text{Bi}_{1-x}\text{Tm}_x\text{FeO}_3$: $x = 0$ (1), $x = 0.0$ (2), $x = 0.10$ (3), $x = 0.20$ (4).

Figures 3,4 show temperature dependencies of temperature conductivity η and thermal conductivity λ of $\text{Bi}_{1-x}\text{Tm}_x\text{FeO}_3$ specimens in the temperature range of 300–1200 K. The dependencies of $\eta(T)$ and $\lambda(T)$ demonstrate anomalies in the range of temperatures of ferroelectric $T_c \sim 1093$ K and antiferromagnetic $T_N \sim 643$ K phase transitions.

To analyze temperature dependencies of thermal conductivity and temperature conductivity, we calculate the free path length of phonon using the known relationship $\eta = (1/3)C_v v_s l_{ph}$ and Debye expression for phonon thermal conductivity $\lambda_{ph} = (1/3)C_v v_s l_{ph}$ (where λ_{ph} — thermal conductivity, C_v — heat capacity of unit volume). Values of η , λ_{ph} and C_p ($C_p \approx C_v$) are determined experimentally (see Fig. 2–4), the sound velocity data is taken from [10]. Independent estimates of l_{ph} from measurements of thermal conductivity and temperature conductivity give the same value of $l_{ph} \sim 3.2 \text{ \AA}$ (at $T > T_N$) and its temperature dependence, which is represented in the insert in Fig. 3.

Thus, the scattering of phonons at crystal grain boundaries can be neglected, if the crystal grains have sizes about several μm , because $l_{ph} \ll d$, where d — mean size of granules. From this, we can make an assumption that structural distortions (i.e. centers of scattering) limiting the free path length of phonons in BiFeO_3 -based multiferroics have values of about lattice spacing. These scattering centers can be local lattice distortions, in particular the distortions of FeO_6 oxygen octahedrons having the nature of Jahn-Teller distortions, which are changed significantly at phase transitions, as well as under external impact [11]. These distortions can play a pivotal role in restricting the phonon heat transfer in these materials.

As can be seen from Fig. 3, in the temperature range of $T_N < T < T_c$ the heating of pure BiFeO_3 demonstrates a little decrease in temperature conductivity, which may be caused by the increase in centers of phonon scattering due

to lattice distortions with temperature growth. According to the information on neutron diffraction in [12], these centers can be the distortions of lattice parameters and changes in volume of the unit cell caused by rotation of oxygen octahedrons (bond angle between neighboring octahedrons of FeO_6 increases) and polar shifts of Bi^{3+} and Fe^{3+} ions from their initial positions as approaching T_c .

In the range of ferroelectric phase transition ($T_c \sim 1093$ K) for BiFeO_3 a minimum of temperature conductivity is observed (Fig. 3), which is a consequence of both the change in sound velocity and the change in free path length of phonon, because $\eta \sim v_s l_{ph}$. It is known that in the region of ferroelectric transition there is a minimum of sound velocity and a peak of sound absorption, which is caused by the interaction between the strain (associated with the sound wave) and the spontaneous polarization (relaxation absorption) and the interaction between the

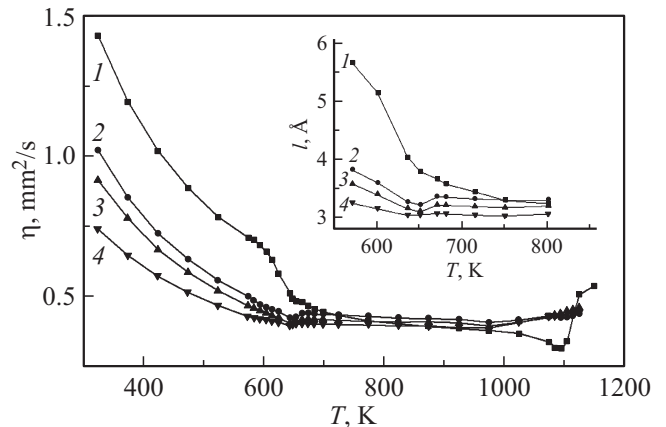


Figure 3. Temperature dependence of temperature conductivity η of $\text{Bi}_{1-x}\text{Tm}_x\text{FeO}_3$ multiferroic: $x = 0$ (1), $x = 0.05$ (2), $x = 0.10$ (3), $x = 0.20$ (4). The insert shows temperature dependence of phonon free path for $\text{Bi}_{1-x}\text{Tm}_x\text{FeO}_3$ multiferroic: $x = 0$ (1), $x = 0.05$ (2), $x = 0.10$ (3), $x = 0.20$ (4).

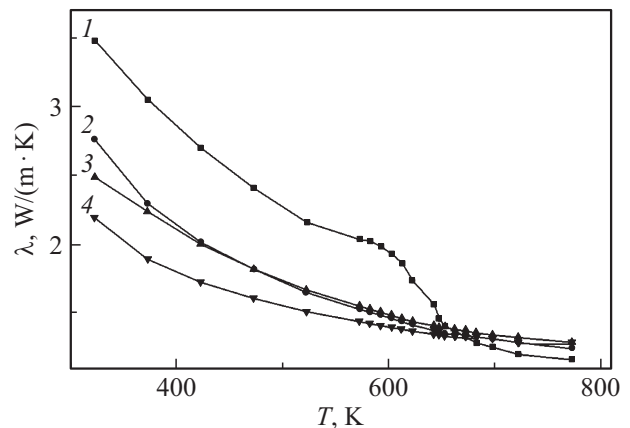


Figure 4. Temperature dependence of thermal conductivity λ of multiferroic $\text{Bi}_{1-x}\text{Tm}_x\text{FeO}_3$: $x = 0$ (1), $x = 0.05$ (2), $x = 0.10$ (3), $x = 0.20$ (4).

sound wave and thermal fluctuations of the polarization (fluctuation absorption) [13].

It can be seen in Fig. 3, that the minimum of the $\eta(T)$ dependence for $\text{Bi}_{1-x}\text{Tm}_x\text{FeO}_3$ compounds in the region of ferroelectric phase transition is getting fuzzy. It may be related to the fact, that with the replacement of bismuth by thulium static distortions of the lattice take place, which cause emergence of local strains and an appropriate polarization related to the piezoelectric effect. Due to the far-reaching nature of elastic and Coulomb forces, the presence of strained polarized areas comes out as an internal shifting electric field, which makes fuzzy the transition. It follows therefrom that the doping with thulium suppresses lattice distortions in the region of T_c related to the shift of oxygen octahedrons and ions of Bi and Fe, which results in decrease in phonon scattering.

With $T > T_c$ in the apolar $Pbnm$ phase, the octahedrons of FeO_6 become regular, polar shifts disappear [14], and an abrupt lattice contraction takes place [14,15]. All of this results in a significant decrease in lattice distortions, i.e. centers of scattering, and thus in an abrupt growth of free path length of phonons and a considerable increase in temperature conductivity in the region of $T \geq T_c$ (see Fig. 3).

It can be seen in Figures 3 and 4 that at $T \leq T_N$ the temperature conductivity and thermal conductivity of specimens grow with decrease in temperature, which is typical for dielectric magnetic materials and is caused by the abruptly grown mean free path length of phonons (see insert in Fig.3), because the transition to magnetically ordered phase usually is accompanied by release of Jahn-Teller distortions (below T_N the electron-lattice interaction is suppressed by the ordered system of spins) [16] and lattice contraction [17]. In the region of antiferromagnetic transition T_N of $\text{Bi}_{1-x}\text{Tm}_x\text{FeO}_3$ compound minima are observed on the $\eta(T)$ and $\lambda(T)$ dependencies. The emergence of minimum in the bismuth ferrite doped with thulium in the region of transition T_N may be caused by the decrease in l_{ph} as a consequence of the phonon scattering amplification on fluctuations of the magnetic parameter of order (due to the existence of spins of rare-earth elements) [18].

The decrease in thermal conductivity of $\text{Bi}_{1-x}\text{Tm}_x\text{FeO}_3$ below T_N (Fig. 3) is related to the fact, that additional local distortions of the crystal lattice appear (i.e. centers of phonon scattering) due to the substitution of bismuth ions by thulium ions with smaller radius.

4. Conclusion

The results of performed studies and their analysis together with the data from literature devoted to structural and acoustic investigations give an evidence that local distortions of the crystal lattice act as the main mechanism of phonon scattering, being caused by the distortions of oxygen octahedrons of FeO_6 and polar shifts of Bi^{3+} and Fe^{3+} ions from their initial positions. It is found that doping with thulium, a rare-earth element, results

in a significant change in temperature anomalies of heat capacity, temperature conductivity, and thermal conductivity in the range of high temperatures. An additional anomaly, specific to the phase transition, is detected at $T = 580$ K in temperature dependencies of heat capacity for compounds with $x \geq 0.10$.

Conflict of interest

The authors declare that they have no conflict of interest.

References

- [1] G.A. Smolenskii, V.M. Yudin. *Sov. Phys. Solid State* **6**, 2936 (1965).
- [2] G. Catalan, F. Scott. *Adv. Mater* **21**, 2463 (2009).
- [3] O. Kuz, Yu. Prots, L. Vasylechko. *Solid State Phenomena* **200**, 100 (2013).
- [4] Krishna Auromun, R.N.P. Choudhary. *Ceram. Int.* **200**, 20762 (2019).
- [5] S.N. Kallaev, A.G. Bakmaev, L.A. Reznichenko, *Letters to the Journal of Experimental and Theoretical Physics* **97**, 541 (2013) (in Russian).
- [6] S.N. Kallaev, Z.M. Omarov, A.R. Bilalov, A.Ya. Kurbataev, L.A. Reznichenko, S.V. Khasbulatov, R.M. Ferzilaev, *Physics of the Solid State* **60**, 9, 1811 (2018) (in Russian).
- [7] S.N. Kallaev, Z.M. Omarov, A.G. Bakmaev, R.G. Mitarov, L.A. Reznichenko, K. Bormanis. *J. Alloys Comp.* **695**, 3044 (2017).
- [8] A.A. Pavlenko, S.V. Khasbulatov, L.A. Shilkina, L.A. Reznichenko, G.G. Gadzhiyev, A.G. Bakmaev, V.A. Alyoshin, *Proceedings of the III International Symposium (LFPM-2014)* **1**, Rostov-on-Don. (2014). 349 p. (in Russian).
- [9] S.V. Khasbulatov, A.A. Pavlenko, L.A. Shilkina, G.G. Gadzhiyev, Z.M. Omarov, A.G. Bakmaev, V.A. Alyoshin, L.A. Reznichenko, *Materials of the International Scientific-Tech. Conference (INTERMATIC — 2016)* **3**, M., (2016). 69 p. (in Russian).
- [10] E.P. Smirnova, A. Sotnicov, S. Ktitorov, N. Zaitseva, H. Schmidt, M. Weihnacht. *Eur. Phys. J.* **83**, 39 (2011).
- [11] P.G. Radaelli, M. Marezio, H.Y. Hwang, S.W. Cheong. *Phys. Rev.* **54**, 8992 (1996).
- [12] D.C. Arnold, K.S. Knight, F.D. Morrison, P. Lightfoot. *Phys. Rev. Lett.* **102**, 027602 (2009).
- [13] R. Blunts, B. Zheksh, *Ferroelectrics and antiferroelectrics*, Mir, M. (1975). 398 p. (in Russian).
- [14] S.M. Selbach, Th. Tybell, M.-A. Einarsrud, T. Grande. *J. Solid State Chem.* **183**, 1205 (2010).
- [15] A.A. Amirov, A.B. Batdalov, S.N. Kallaev, Z.M. Omarov, I.A. Verbenko, O.N. Razumovskaya, L.A. Reznichenko, L.A. Shilkina, *Physics of the Solid State* **51**, 6, 1123 (2009) (in Russian).
- [16] G. Catalan, F. Scott. *Adv. Mater* **21**, 2463 (2009).
- [17] H. Fujishiro, S. Sugavara, M. Ikebe. *Physica B* **316–317**, 331 (2002).
- [18] M. Ikebe, H. Fujishiro, Y. Konno. *J. Phys. Soc. Jpn.* **67**, 4, 1083 (1998).